Perfect Circles: A Study of the Scattering Regions of Wolf Rayet Binary Stars

Stella Yoos[1], Jennifer Hoffman[2], and Andrew Fullard[2]
[1]Student Contributor, University of Denver, Denver, CO
[2]Advisor, Department of Physics and Astronomy, University of Denver, Denver, CO

Abstract

Although we have been able to develop an understanding of many aspects of stellar evolution and formation, a few key gaps remain. One is the fate of massive binary star systems composed of Wolf-Rayet (WR) and O-type stars. In these WR + O binaries, the stellar winds surrounding these stars collide, creating a complex interaction region in which light from the stars scatters and becomes polarized. To study these scattering regions, I employ a technique that allows me to map the polarization of the light emitted from these stars and track its variation over the binary orbit. I found that although we have some models for this behavior, they do not fully reproduce the observed data, suggesting these systems are more complex that previously known. The unexplained behaviors give clues to the complexity of these systems and shows how these models can be improved upon in the future. Understanding the structure and evolution of this scattering region could be the key to understanding the lives and eventual deaths of these stars.

Keywords: Binary star systems – spectropolarimetry – astronomy – polarization – Wolf-Rayet Binaries

1 INTRODUCTION

Although up to 85% of stars exist with companion stars, in stellar systems known as binaries, many of these star systems are not well understood[1]. Their evolution and ultimate fate can be dramatically altered by existing in a binary, especially in cases where matter is being exchanged between the stars.

One of these types of star systems involves the pairing of a Wolf-Rayet (WR) star, which is an evolved massive star that has a particularly active stellar wind, and an O-type star, which is a massive main-sequence star, upwards of 15 times the mass of the sun (Crowther 2007). A main-sequence star is one that is still undergoing nuclear fusion in the core of the star, like our Sun, and can be thought of as the middle, stable, period of a star's life. The small distance between the stars and the exchange of mass due to the stellar winds creates what is known as a scattering region – a cloud of gas and dust in and around the system. Some of the light we observe from these stars may have been scattered by this material.

This scattering region can be measured and observed several different ways. One of these ways is through polarimetry, which is a technique that measures the orientation of light coming from interstellar objects. Polarization can be thought of as the preferred direction of the light. As shown in Figure 1, in a perfectly spherical scattering region the polarization vectors cancel, yielding no intrinsic polarization, or no preferred direction of the light. However, if the scattering region is elongated, we measure a net polarization and its position angle can tell us the direction in which the scattering region is elongated. Another way to characterize these objects is to observe their chemical makeup, or spectrum – again through the light they emit. The combination of these techniques yields spectropolarimetry, which helps to paint a more complete portrait of the system. We used the Robert Stobie Spectrograph (RSS) spectropolarimeter on the 11-m Southern African Large Telescope (SALT) to obtain spectropolarimetric data on several of these WR + O star binary systems. I focus here on two of these systems, WR 42 and WR 79. These two stars have nearly the same period – which is the amount of time it takes for the stars to complete one full orbit around each other.

Both systems also contain almost identical stars, each having a WC7 star and a O5-8 star, both of which are specific designations of their respective star types. An O5-8 star is a massive main sequence star that is slightly cooler than the hottest stars known. A WC, or Wolf-Rayet carbon star, is categorized by the presence of strong carbon emission lines from the hot stellar

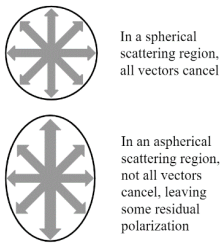

Figure 1. Polarization Vectors. A depiction of spherical (top) and aspherical (bottom) scattering regions.

winds (Crowther 2007). Some of these emission lines are shown in the top panel of Figure 2.

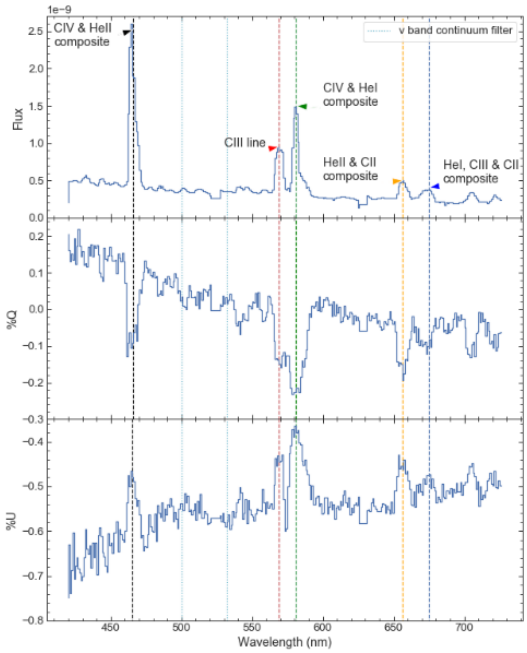

Figure 2. Flux, %Q, and %U vs Wavelength of WR 79. This is a single-phase graph of 0.999 phase, showing the flux, %Q, and %U against wavelength. Several carbon emission lines are identified as well as the region for the continuum filter

These two stars differ primarily in their inclination angle, which is the angle at which the system is tilted relative to our viewpoint. This makes them excellent candidates for determining the underlying structure of these objects, since their differences can be largely attributed to the different angles at which we view the two systems.

2 METHODS

We receive polarized spectra from SALT on each of our two binaries. Each spectrum measures the observed polarization at each wavelength between 400 and 700 nanometers with a resolution of 0.1 nm. We convert this spectrum to a more usable form by applying various filters using Python. These filters reduce regions, or bins, of the data into a single point, and from this reduction we can produce Stokes parameters. These parameters can be thought of as a polarization coordinate system that allow us to map the data onto physical parameters. We also perform a calculation for orbital phase, which is the positioning of the stars in their orbits at the time they were observed. By calculating this phase, we are able to observe how the star and its polarization evolves as the stars rotate around each other.

The filter calculation returns two Stokes parameters, %Q and %U. Stokes parameters can be thought of as a kind of coordinate system, where a higher %U indicates more polarization at 45 and 135 degrees, and a higher %Q indicates the same at 0 and 90 degrees. I can plot the variations of these basic parameters using Python scripts. These graphs tell us about how the polarization of the system varies as a function of orbital phase, or the position of the stars in their orbit. These graphs can also tell us about the structure of the scattering material. For example, if one star exhibits a higher level of polarization in %Q, then likely there is more scattering material elongated at that angle (0 and 90 degrees on the sky).

One of the ways we analyze this data is in the form of continuum polarization. This can be thought of as the polarization of the spectral regions in between the emission lines, which arise from the stellar surfaces. The filters we use return three different bands – b band, which is centered around 427 nm, v band (516 nm), and r band (600 nm). The data has a higher uncertainty near the edges of the detected spectrum, so we primarily focus on the v-band. Using these continuum regions allows us to avoid polarization from the carbon lines, which likely exhibit different behavior. The largest contribution to the continuum polarization is O-star light scattering off the WR wind. Figure 3 shows a computer model of this scattering region in the WR + O binary V444 Cygni, with the O-star rotating around the WR creating a bow-shock region. This model of the scattering region of V444 Cygni can help give us an idea of what the scattering regions could look like for WR 42 and WR 79, as well as identify some of the features present in the continuum polarization.

When we examine these graphs of polarized light, inherently they contain some extraneous polarization – polarization not originating from the star system. Aside from instrumental error, the strongest extraneous contributor is interstellar polarization (ISP), caused by light scattering in the gas and dust between us and the object being observed. Previous studies of WR 42 and WR 79 done by Moffat et al. have estimated the ISP contribution for these stars, which we adopt here (Moffat et al. 1993). By subtracting those estimates for interstellar polarization from our SALT data, we can get a better sense of what the intrinsic polarization of these stars is,

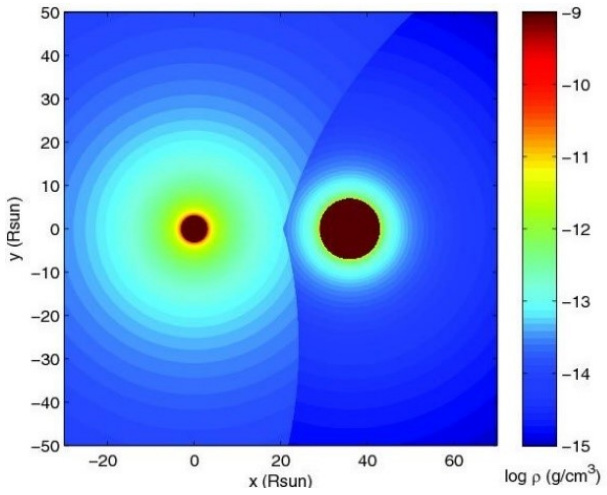

Figure 3. WR + O Scattering Region. A computer model of the wind scattering region between the WR star (left) and the O-star(right) in the WR+O binary V444 Cygni (Lomax et al. 2015)[2]

which is critical to understanding the scattering region.

Current models of these WR + O systems assume that the scattering region that surrounds the system of stars is ellipsoidal Brown et al. 1978[3], hereafter BME). Although this is a simple model, it has proven to be accurate when considering continuum polarization. It predicts the continuum polarization should behave roughly sinusoidally with phase. This periodic behavior has been observed by St. Louis et al.[4] for both WR 42 and 79. Non-sinusoidal behaviors may occur when evaluating line polarization, which is outside the scope of this paper.

The BME model assumes that both stars are point sources, or that they can be approximated as massless and size-less dots, and that the ellipsoidal scattering region is centered around one star and is optically thin, meaning it has a low density. Both are simplifications but can still provide us with an idea of the scattering region and the evolution of these star systems, without making calculations immensely complicated. From these base assumptions, the authors derive an analytical formula to describe the polarization variation with phase. In this formula, q_0, q_3, q_4, u_0, u_3, and u_4 are dependent variables and phase is an independent variable.

$$q = q_0 + q_3 cos(4\pi * Phase) + q_4 sin(4\pi * Phase) \quad (1)$$

$$u = u_0 + u_3 cos(4\pi * Phase) + u_4 sin(4\pi * Phase) \quad (2)$$

Using Python, I performed least squares fits to compare this theoretical sinusoidal curve with our SALT data for WR 42 and WR 79. The Stokes parameters returned by this model can be manipulated and graphed in the same ways as the original Stokes parameters and provide a hypothetical picture of the scattering region to compare our results with.

The BME model also provides us with some properties of the system, namely the inclination angle (i) which is the angle at which we view the system, omega (Ω) which is how the orbit is projected onto the sky, and lambda$_2$ (λ_2), which is the angle of the distribution of material in the scattering region as measured from the line between the stars. These parameters are further explained in Figure 4. The inclination angle is calculated as follows:

$$x = \frac{(u_3 + q_4)^2 + (u_4 - q_3)^2}{(u_4 + q_3)^2 + (u_3 - q_4)^2} \quad (3)$$

$$i = cos^{-1}\left(\frac{x^{\frac{1}{4}} - 1}{-x^{\frac{1}{4}} - 1}\right) \quad (4)$$

Following the algebra from Drissen et al.[5], I calculated the values for Ω and λ_2 for my two binaries.

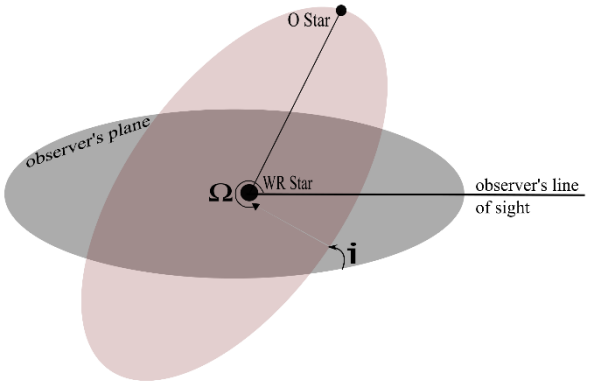

Figure 4. Orbital Properties. In this figure, the ecliptic plane lies along our line of sight. i is the angle between the ecliptic plane and the plane of the orbit of the O-Star. Omega (Ω) is the angle of the O-star's orbit projected onto the sky.

Any deviations from this theoretical model could indicate that the initial assumption of a symmetric ellipsoidal scattering region was an incomplete picture. For example, the WR star wind might have a more complex geometry, or scattering might occur in regions other than the WR wind[6]. The presence of behavior consistent with an aspherical scattering region could indicate that our current model and understanding of these WR + O binaries is not complete, or that some of the simplifying assumptions made are not as close an approximation as hoped.

A previous study of these two objects by SL87 provides us a point of comparison for our data. Their data utilized a wide b-band filter for the continuum data and exhibits a close match to the BME fit.

Since the polarization across the three continuum bands is very similar, we combined the data from all three filters in an error-weighted average. This reduces

uncertainties on the measured values and allows us to do a more direct comparison of our data with the SL87 data, as the error-weighted average is closer to the filter than any of our individual data. Additionally, since electron scattering is spectrally grey—meaning it doesn't change with wavelength—performing this error weighted average does not lose any spectral information.

3 RESULTS

Figures 5 and 6 show the error weighted average of the SALT data for WR 42 and WR 79 respectively compared with the continuum data from St. Louis et al. (SL87)[4].

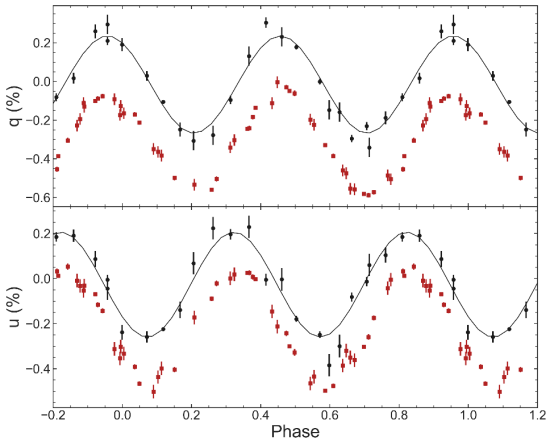

Figure 5. WR 42 Error-Weighted Average Comparison with BME Fit. Displays the error weighted average (black circles) continuum polarization of WR 42 and compares it with the wide b-band polarization (red squares) data from St. Louis et al[4]. The black curve is the BME curve fit to the error weighted average following ISP Subtraction. The St. Louis data has been phase shifted by +0.09.

Their data is used as a point of comparison because of the low systematic error present, and because they have a significant amount of data on these objects. Tables 1 and 2 display the BME parameters calculated for the SALT WR 79 and SALT WR 42 data respectively. These values are used for the calculations of the three primary parameters: i, Ω, and λ_2.

The SALT data for WR 42 tends to have more variability in both %q and %u, although the fit calculated from this data does match the SL87 data well. WR 79 exhibits less variation from this theoretical curve; almost all data points lie on the curve, within their uncertainties. It is worth noting that WR 79 is a brighter star system, which greatly improves our ability to accurately observe this object. Further comparison of the two data sets reveals slight phase offsets for both stars. WR 79 requires an additional 0.04 phase, and WR 42 requires an additional 0.09 phase. In order to align our data with that of SL87,

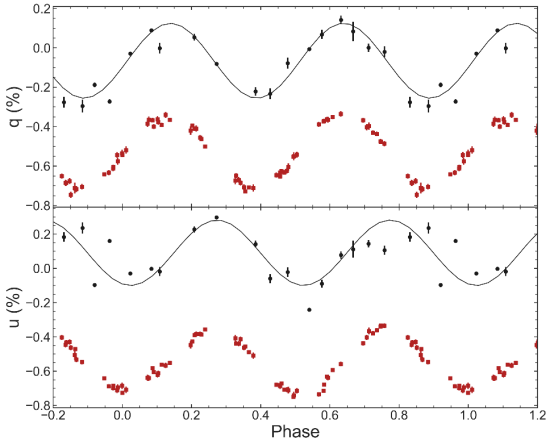

Figure 6. WR 79 Error Weighted Average Comparison. The same but for WR 79. The St. Louis data has been phase shifted by +0.04.

we added constant phase offsets to the SL87 data (0.09 for WR 42 and 0.04 for WR 79). This phase shift could be due to a gradual change in the orbital period of each system as the stars exchange mass, or the result of uncertainty in the phase calculations. Also, worth noting is the slight phase offset between %q and %u for each star across all bands. This offset may indicate a minor asymmetry in the distribution of scattering material in the systems. This average also exhibits strong periodic behavior in both %q and %u for both star systems. In particular, the error weighted average for WR 42 returns data that more closely matches previously observed trends than the individual bands do. By contrast, in WR 79 it appears to have further exaggerated the differences in %q and %u. Table 3 shows the calculated primary parameters for the BME fit based upon our error-weighted average data for each star, while Table 4 shows the same parameters calculated by SL87. Our values for inclination angle agree within uncertainties with those from SL87. The values for Ω and λ_2 for WR 42 are consistent with those calculated by SL87.

Interestingly, WR 79 presents quite different results for both Ω and λ_2. The uncertainty estimates we used are based on Wolinski & Dolan[7]. This method includes the inherent biases in polarimetry that the fit errors cannot include because they are synthetic. The dominant contributors to these estimates are systematic instrumental uncertainties, not uncertainties due to the curve fitting. Because Wolinski & Dolan developed their prescription after SL87 published their data, the error estimates in the SL87 data do not include correct error estimates for Ω and λ_2[7]. An increase in the uncertainties on the SL87 parameters for WR 79 may allow for my parameter fit results to match within error.

Table 1 BME parameter values for WR 79. These are the BME parameters returned for the SALT WR 79 data following an ISP subtraction

q0	–0.065 ± 0.003	u0	0.091 ± 0.003
q3	-0.034 ± 0.004	u3	–0.182 ± 0.004
q4	–0.130 ± 0.005	u4	–0.057 ± 0.005

Table 2 BME parameter values for WR 42. The same as in Table 1, except for WR 42.

q0	–0.016 ± 0.005	u0	–0.027 ± 0.005
q3	0.216 ± 0.007	u3	–0.143 ± 0.007
q4	–0.130 ± 0.007	u4	–0.184 ± 0.007

4 DISCUSSION AND CONCLUSION

Although our data match the BME model quite well generally, there are some slight deviations worth noting. These could indicate that some of the base assumptions we made in applying this model are inaccurate. The BME model assumes a low-density scattering region around the system, which implies low-density winds for both the O star and the WR star. WR stars are known to have very dense, opaque winds (Crowther 2007), so the deviations present in our data from the model's predicted curve are likely due to a higher density scattering region than allowed for in the model.

Figures 5 and 6 also show that the average values for %q and %u are not centered at zero polarization. There are two primary reasons that we may have some constant intrinsic polarization: the first is that we may not be subtracting all the interstellar polarization, and the second is that there is an additional elongated scattering region in the system that is not accounted for by the BME model. In my future work on these binaries, I will investigate both these scenarios.

The previous study done on these objects by SL87 provides a standard to which we can compare our results. Their study investigating the polarimetric behavior of WR + O binary systems reveals a similar sinusoidal trend that largely matches the BME model. Additionally, they have a large dataset and low systematic error, which makes it a good point of comparison for our data obtained from SALT. The error-weighted average of the three bands of our data does not exactly correspond to the SL87 results; both stars required a slight phase offset to match the SL87 data. Given the amount of time between the different observation periods and the uncertainty of the phase calculations, it is reasonable to infer that slight changes in the orbit or circumstellar material configuration have occurred between the two datasets.

Some of the discrepancies between our values for i, Ω, and λ_2, and the ones obtained by SL87 can be explained in part by the different filters used to acquire the data. SL87 used a wide blue filter centered at 470 nm with a width of 180 nm. In a WC7 star like WR 79 or WR 42, this filter covers the 465 nm/468 nm line region, which is the strongest emission line present in these stars. Since this filter works to essentially obtain an average value of polarization for that spectra, if this line were highly polarized, it would pollute the "continuum" data.

Wolinksi & Dolan[7] showed that when measurement uncertainties become significant, the BME model returns an over-estimation of the value for the inclination angle. In our case, this effect is exacerbated by our relatively sparse data points over the orbital cycle. Since all further calculations are based upon this initial value for i, any error introduced here will be further amplified. This may help to explain the difference between our calculated fit parameters and those found by SL87.

Although the BME model of the scattering regions of these stars can provide a basic model of their behavior, it is not able to fully capture the complex nature of the stellar winds. Deviations from this hypothesis are present in the phase shift between %q and %u, as well as in the inconsistent values for the inherent properties in the stars. These deviations may indicate that there is some intrinsic polarization caused within the system itself and that the scattering region around this system is much denser than assumed.

Though a look at the continuum polarization of these star systems can provide a glimpse into their basic structure and evolution, more detailed observations and conclusions can be drawn through examination of their line polarization and interstellar polarization. We have a method of extracting polarization within the strong emission lines, which are known to exhibit different behavior than the continuum in these binaries. In the next step of this project, I will compare these emission lines with the continuum and with each other. Through this analysis, we can begin to map the wind interaction regions to provide a clearer picture of the life of these stars.

This research indicates that our current model for the behavior of these systems is incomplete. To better capture the nature and evolution of these scattering regions, and of these binary systems, we need a model allowing for dense stellar winds and for polarization

Table 3 RSS/SALT BME Parameters. Binary system parameters derived from the BME fit to the error-weighted average of the three continuum polarization bands for each star.

	WR 42	**WR 79**
Inclination Angle (i)	53°± 6.3°	55°± 3.9°
Omega (Ω)	-46°± 20°	-29°± 15°
Lambda_2 (λ_2)	-29°± 10°	3°± 9°

Table 4 St. Louis BME Parameters. Binary system parameters derived by SL87 from their wide b-band continuum polarization.

	WR 42	**WR 79**
Inclination Angle (i)	43.5°± 5°	44.8°± 5°
Omega (Ω)	-43.8°± 9.3°	34.4°± 8°
Lambda_2 (λ_2)	-26.5°± 5.7°	-44.8°± 3.6°

arising from light scattering in the WR wind. Further analysis of these binaries using line polarization will help to determine possible structures of those scattering regions and provide insight into how changing stellar wind densities and polarizations affect the life of these stars.

5 EDITOR'S NOTES

This article was peer reviewed.

REFERENCES

[1] CSIRO Australia Telescope National Facility & NSW, E. Introduction to Binary Stars (2019). URL `https://www.atnf.csiro.au/outreach/education/senior/astrophysics/binary{_}intro.html`.

[2] Lomax, J. R. *et al.* V444 Cygni X-ray and polarimetric variability: Radiative and Coriolis forces shape the wind collision region. *Astronomy and Astrophysics* (2015). `1410.6117`.

[3] Brown, J. & Fox, G. K. Polarisation by Thomas Scattering in Optically Thin Stellar Envelopes. *Astronomy and Astrophysics* (1978).

[4] St.-Louis, N., Drissen, L., Moffat, A. F. J., Bastien, P. & Tapia, S. Polarization variability among Wolf-Rayet stars. I. Linear polarization of a complete sample of southern Galactic WC stars. *The Astrophysical Journal* (1987).

[5] Drissen, L., Lamontagne, R., Moffat, A. F. J., Bastien, P. & Seguin, M. Spectroscopic and polarimetric parameters of the runaway WN7 binary system HD 197406 - Is the secondary an X-ray-quiet black hole? *The Astrophysical Journal* (1986).

[6] Villar-Sbaffi, A., St-Louis, N., Moffat, A. F. J. & Piirola, V. First Ever Polarimetric Detection of a Wind-Wind Interaction Region and a Misaligned Flattening of the Wind in the Wolf-Rayet Binary CQ Cephei. *The Astrophysical Journal* (2005).

[7] Wolinski, K. G. & Dolan, J. R. Confidence intervals for orbital parameters determined polarimetrically. *Monthly Notices of the Royal Astronomical Society* (1994).